2018

Enhancing FRP-to-concrete Bond Behavior by Epoxy Ribs

Cheng Jiang

Baolin Wan

John Omboko

Enhancing FRP-to-concrete Bond Behavior by Epoxy Ribs

Cheng Jiang, Baolin Wan and John Omboko

Synopsis: The bond between external bonding (EB) of fiber reinforced polymer (FRP) composite materials to concrete is the weakest link in the strengthened concrete flexural members. There are three mechanisms to transfer the interfacial shear between FRP and the concrete substrate, i.e., adhesion, interlocking and friction. This paper proposes a new approach by grooving on the concrete surface before applying epoxy to make epoxy ribs to increase interlocking. An experimental program was conducted to verify the effectiveness of the proposed epoxy ribs. Six grooves perpendicular to the fiber direction were cut on the bonding surface of the concrete blocks. The grooves were filled by wax in the unfilled specimens and with epoxy primer in the epoxy filled specimens before CFRP plate was installed. The experimental results show that epoxy-filled grooves can significantly improve the bond between FRP and concrete.

Keywords: concrete; FRP; bond; grooving; epoxy rib; bond-slip relationship

Cheng Jiang is currently a Postdoctoral Fellow at The Hong Kong Polytechnic University, Hong Kong SAR, China. He obtained his Ph.D. degree from City University of Hong Kong. He worked as a visiting scholar at Marquette University from 2016 to 2017. His research interests encompass structural rehabilitation, composite structures, and FRP applications.

ACI member of **Baolin Wan** is an associate professor in the Department of Civil, Construction and Environmental Engineering at Marquette University, Milwaukee, WI. He is an associate member of ACI Committee 440, Fiber-Reinforced Polymer (FRP) Reinforcement. His research interests include use of FRP in structural members, numerical and experimental modeling of repaired and retrofitted structures, field testing and nondestructive evaluation of bridges, behavior of reinforced and prestressed concrete structural elements, and finite element analysis.

John Omboko is a former research assistant at Marquette University, Milwaukee, WI. He received his MS in civil engineering from Marquette University in 2017.

INTRODUCTION

Structural rehabilitation by externally bonded (EB) fiber reinforced polymer (FRP) composite material is widely adopted, largely due to its advantages of lightweight, high strength, and excellent durability [1-4]. The interfacial bond behavior between FRP and concrete is the weakest link in the retrofitted system of concrete members. For a composite structure combining two mechanically connected bodies, there are in total three mechanisms to transfer the interfacial shear stress between FRP and concrete, i.e., adhesion, interlocking (or dowel action) and friction. To solve the debonding issue and enhance the FRP-to-concrete bond behavior, researchers have suggested different methodologies based on these three mechanisms [5-10].

This study aims to find a novel, reasonable and effective method to enhance the interfacial bond behavior between FRP and concrete by improving interlocking effect without cutting the FRP and minimizing the damage of concrete. In order to increase the interlocking mechanism, strong "ribs" in the adhesive layer can be formed by grooving on the surface of concrete substrate before applying the epoxy. An experimental program was conducted in this study to test the FRP bonded concrete specimens with and without epoxy ribs to verify the effectiveness of this proposed approach.

RESEARCH SIGNIFICANCE

Epoxy ribs were made by filling the pre-cut grooves on the surface of concrete blocks before applying FRP. Single shear pull out test results show that the specimens with epoxy ribs had significant better global response and local bond-slip relationship.

EXPERIMENTAL PROGRAM

Specimen Design

Nine plain concrete blocks with dimensions of 533 mm (length) × 152 mm (width) × 152 (depth) mm (21 in. × 6 in. × 6 in.) were prepared for the bond tests of EB-FRP joints. Six specimens were cut six grooves on the surface of each concrete substrate in transverse direction. The rest three were prepared as regular specimens without grooves. The grooves on the concrete surfaces were designed as 3 mm (0.12 in.) in width and 5 mm (0.20 in.) in depth. The first groove line was marked 75 mm from the edge of the concrete block to accommodate the 25 mm (1 in.) pre-crack condition and the rest of the groove lines were 50 mm (2 in.) apart as shown in Fig. 1.

The nine specimens were divided into three groups. For the six specimens with grooves, three had grooves filled with epoxy and three with wax. The specimen details are listed in Table 1. The specimen ID includes two components divided by "-". "C", "F" and "U", which are the first component in specimen ID, indicate the control specimens, and the specimens with and without epoxy ribs, respectively. The second term of specimen ID shows the number of identical specimens with the same testing conditions.

Materials Properties and Specimen Preparation

A commercial ready-mixed concrete was used to prepare specimens. Seven 152 mm (6 in.) (diameter) × 305 mm (12 in.) (height) concrete cylinders were prepared for measuring the compressive and tensile strengths. The measured concrete compressive strength and split tensile strength at 28 days are listed in Table 2.

All concrete surfaces for bonding FRP were roughening by mechanical grinding. Grooves were made by saw cut for Specimens F and U. After grooving, specimens were cleaned up using high-pressure water together with a steel brush to help eliminate any dirt or dust particles from the grooves and on the surface of the specimens. It also ensured that the specimens were well roughened to achieve a strong bond between FRP and concrete. After cutting and cleaning, the specimens were put in lab environment to dry for at least 24 hours before applying wax, epoxy and FRP.

The grooves of three U specimens (U-1, U-2 and U-3) were filled by soft wax to avoid the penetration of applied epoxy. The wax filling was also conducted at the edges of grooves in the specimens with epoxy interlocking (F-1, F-2 and F-3) which was not covered by FRP. Therefore, the epoxy rib has the same width of FRP. The concrete blocks with grooves and wax filling are shown in Fig. 2.

Carbon FRP plate (Tyfo® UC Laminate Strip) with a nominal thickness of 1.5 mm (0.06 in.) was used in this work. Two kinds of epoxy resin were applied (i.e., Tyfo® S and Tyfo® TC). Tyfo® S was applied as a prime coat before applying a layer of Tyfo® TC to the substrate. The cleaned FRP plate with Tyfo® TC was then bonded to the concrete substrate. By this way, the epoxy ribs were formed for the specimen F-1, F-2 and F-3. The U specimens were made with the same conditions but with the wax instead of the epoxy ribs. The control specimens without grooves were also made by following same procedure. The mechanical properties of the FRP plate and two kinds of epoxy are listed in Table 2.

Test Setup and Instrumentation

A single shear pull-out test was adopted to evaluate the bond behavior of the EB-FRP joints in this work. The pull load was applied horizontally and parallel to the FRP fiber direction by a MTS actuator (Fig. 3). Conventional electric strain gages were installed on the FRP for each specimen to measure the strain on the FRP at different locations and calculate the experimental bond-slip relationships. The first strain gage was attached on the unbonded region of the FRP and the second one was installed at the location where FRP started to be bonded (25 mm (1 in.) from the edge of concrete block as shown in Fig. 4). The rest of strain gages were 25 mm (1 in.) apart as shown in Fig. 4. One linear variable differential transformer (LVDT) was mounted on one side of the concrete substrate to measure the relative displacement between FRP and concrete at the location of the pre-crack tip. All specimens were tested with displacement control at a loading rate of 0.0127 mm/s.

TEST RESULTS AND DISCUSSION

Failure Modes and Global Responses

All specimens were loaded monotonically until suddenly failed with a thin layer of concrete skin pulling off from the concrete substrate. The typical failure modes are shown in Fig. 5. It can be observed that the thickness of damaged concrete of the specimens with epoxy ribs was larger than that of control and U specimens. More concrete crushed near the epoxy ribs. The bond strengths (peak loads) in the tests are listed in Table 1. The load vs. relative displacement relationships at loaded end for the EB-FRP joints are shown in Fig. 6.

Two of control specimens were damaged without recorded data due to testing errors. The bond strength of the only successfully tested control specimen was 34.0 kN (7.6 kips). Specimens using the same FRP and epoxy, and similar concrete as the control specimens tested by another researcher [11] had similar bond strengths and damage mode. Therefore, the behavior of C-1 can represent the specimens without grooves.

The load vs. displacement behaviors of U specimens are similar to that control specimen as shown in Fig. 6. The average bond strength of U specimens was 33.0 kN (7.4 kips), which is also similar to that of control specimen. For the specimens with epoxy ribs (i.e., F-1, F-2 and F-3), the bond strength with 62.3 kN (14.0 kips) of average strength shows a stable level and is 83% and 89% higher than that of control specimen and U specimens, respectively. However, the load-displacement curves of specimens with epoxy ribs show larger scatter (Fig. 6) due to the effect of

epoxy interlocking and the non-uniformity of concrete material. Not all epoxy ribs contribute the same amount of resistance when the load is increased and the debonding crack propagates from the loaded end to the free end. Meanwhile, concrete is a non-uniform composite material. Wall effect [12-13] of concrete, which means smaller aggregates concentrate near the surface of the concrete specimen, leads to higher non-uniformity of surface concrete near the epoxy ribs. Therefore, the load-displacement curves show large differences in the three filled (F) specimens. However, the bond strengths are similar because there are totally six ribs in each specimen and the overall interlocking effect should not have large variation.

The comparison of strain distribution at different loaded end slips (s_0) between U specimens and F specimens are illustrated in Fig. 7. The strain values in this figure are the average of three specimens in each type of specimen when they have same slips (s_0). The cases of s_0 = 0.1 mm and 0.2 mm (0.0039 in. and 0.0079 in.) indicate the moments when the load has not reached the peak (or turning) load yet (see Fig. 6). Meanwhile, the cases of s_0 = 0.3 mm and 0.4 mm (0.0118 in. and 0.0157 in.) refer to the later loading periods before failure. At beginning, there are significant strain gradients which means the interfaces did not have any debonding. On the contrary, the similar strain values along the FRP indicate the debonding between FRP and concrete. It can be concluded from Fig. 7 that the F specimens had much higher FRP strains than U specimens before the failure of the specimens. Therefore, the high strength of FRP material was used due to the epoxy interlocking.

Bond-slip relationship

The bond-slip relationship is essential to investigate the macro mechanical properties of EB-FRP specimens. In general, there are two methods to obtain the bond-slip relationship from experimental tests: (1) directly measurement from closely spaced strain gage data; and (2) indirect analytical solutions derived from other experimental response such as load-displacement curves. Both methodologies were undertaken in this work to study the bond-slip relationship. The FRP strain and bond stress can be expressed as:

$$\varepsilon_f(x) = \frac{ds(x)}{dx} \tag{1a}$$

$$\tau(x) = E_f t_f \frac{d\varepsilon_f(x)}{dx} \tag{1b}$$

where E_f and t_f are the elastic modulus and thickness of the FRP plate, respectively; $\varepsilon_f(x)$, $s(x)$ and $\tau(x)$ are the tensile strain, slip and bond stress along the longitudinal direction x at a particular pull force F_i. The local slip of FRP can be calculated using the following equation:

$$s(x) = s_0 - \int_x^{L_f} \varepsilon_f(x) dx \tag{1c}$$

in which s_0 is the displacement at the loaded end, which was measured by LVDT in this study; L_f is the bond length of FRP; and the zero point of x axis is set at the free end. The experimental bond-slip results can be easily calculated using Eq. (1) from the strain gage data in the tests. Fig. 7 shows the experimental bond-slip relationship of all specimens.

On the other hand, the bond-slip relationships can also be inversely derived from the load-displacement curves if the form of bond-slip model is known [14]. A widely adopted bond-slip model is used in this work as Eq. (2) [2,15-16].

$$\tau(s) = \frac{E_f t_f \alpha}{\beta^2} e^{-\frac{s}{\alpha}} \left(1 - e^{-\frac{s}{\alpha}}\right) \tag{2}$$

There are two unknown parameters, α and β, in the bond-slip relationship, which govern the shape of the bond-slip curve. α is the slip at the turning point of the equivalent bilinear load–slip curve; and the reciprocal of β determines the initial tangential rigidity of the load–slip response curve. The more detail explanation can be found in [15]. Based on Eq. (2), the relationship between the external load applied to the FRP, F, and the relative slip between FRP and concrete at the loaded end, s_0, is:

$$F = E_f t_f b_f \frac{\alpha}{\beta}\left(1 - e^{-\frac{s_0}{\alpha}}\right) \quad (3)$$

The unknown coefficients α and β can be obtained by a numerical nonlinear regression analysis using Eq. (3) to fit the experimental load-displacement curves of specimens. As the load-displacement curve is the global response of the EB-FRP joint, the bond-slip relationship obtained by this indirect method is believed to be the average behavior of the FRP-to-concrete interface subjected to in-plane shear [14]. The obtained values of α and β are listed in Table 1 and the fitted curves are drawn as the dotted lines in Fig. 6. By substituting the α and β values into Eq. (2), the bond-slip relationships of specimens can be obtained and plotted in Fig. 8.

It is obvious that the maximum bond stress of the specimens with epoxy ribs is higher than that of U and C specimens in the bond-slip relationships derived from both direct and indirect methods. The obtained α value of specimen with epoxy ribs is much higher than control ones while the values of β are similar. The bond-slip relationships of specimens with epoxy ribs at 75 mm (3 in.) from the loaded end have high residual bond stresses because the bond stresses at that location were calculated from the strain gage data at 50 mm (2 in.) and 100 mm (4 in.) from the loaded end which were exactly at the epoxy rib locations. Hence, the epoxy rib has an enhancing effect on local bond-slip relationship.

CONCLUSIONS

This paper proposes a novel approach to enhance the interfacial bond between externally bonded FRP and concrete. An experimental program was conducted in this work to verify the effectiveness of this method. Both the global response and local bond-slip relationship are enhanced due to epoxy ribs. The bond strength of the specimens with epoxy ribs is 83% and 89% higher than those of control specimen and unfilled specimens, respectively. Such increased strength is attributed to the interlocking provided by the epoxy ribs and the extra bond areas in the grooves. The unfilled specimens had similar behavior and bond strength as control specimen. Therefore, the unfilled grooves do not have significant effect on the bond between FRP and concrete. With both filled and unfilled specimens having the same geometrical features, presence of epoxy ribs in the filled specimens plays a key role in increasing the bond strength between FRP and concrete.

ACKNOWLEDGEMENTS

The first and third authors of this paper obtained financial aids from City University of Hong Kong and Marquette University during the period of this research. The FRP materials were donated by Fyfe Company LLC.

REFERENCES

[1] Wu, Y.F., and Jiang, C., 2013, "Effect of load eccentricity on the stress–strain relationship of FRP-confined concrete columns." Composite Structures, 98, 228-241.

[2] Wu, Y.F., Xu, X.S., Sun, J.B., and Jiang, C., 2012, "Analytical solution for the bond strength of externally bonded reinforcement." Composite Structures, 94(11), 3232-3239.

[3] Yu, Q.Q., and Wu, Y.F., 2017, "Fatigue strengthening of cracked steel beams with different configurations and materials." Journal of Composite for Construction, 21(2): 04016093.

[4] De Lorenzis, L., Miller, B., and Nanni, A., 2001, "Bond of fiber-reinforced polymer laminates to concrete." ACI Material Journal, 98(3), 256-264.

[5] Hosseini, A., and Mostofinejad, D., 2013, "Effect of groove characteristics on CFRP-to-concrete bond behavior of EBROG joints: experimental study using particle image velocimetry (PIV)." Construction and Building Materials, 49, 364-373.

[6] Hosseini, A., and Mostofinejad, D., 2013, "Experimental investigation into bond behavior of CFRP sheets attached to concrete using EBR and EBROG techniques." Composites Part B: Engineering, 51, 130-139.

[7] Kim, S., and Smith, S.T., 2009, "Behaviour of handmade FRP anchors under tensile load in uncracked concrete." Advances in Structural Engineering, 12(6), 845-865.

[8] Bank, L.C., and Arora, D., 2007, "Analysis of RC beams strengthened with mechanically fastened FRP (MF-FRP) strips." Composite Structures, 79(2), 180-191.

[9] Wu, Y.F., and Liu, K., 2013, "Characterization of mechanically enhanced FRP bonding system." Journal of Composites for Construction, 17(1), 34-49.

[10] Wu, Y.F., He, L., and Bank, L., 2015, "Bond-test protocol for plate-to-concrete interface involving all mechanisms." Journal of Composites for Construction, 20(1), 04015022.

[11] Mohammadi T., 2014, "Failure Mechanisms and Key Parameters of FRP Debonding from Cracked Concrete Beams." PhD dissertation, Marquette University, Milwaukee, WI, USA.

[12] Jiang, C., Wu, Y.F., and Jiang, J.F., 2017, "Effect of Aggregate Size on Stress-strain Behavior of Concrete Confined by Fiber Composites." Composite Structures, 168, 851-862.

[13] Neville, A.M., 1996, Properties of concrete. 4th ed. Essex, UK: ELBS Publication, Addison-Wesley Longman Limited.

[14] Dai, J.G., Ueda, T., and Sato, Y., 2005, "Development of the nonlinear bond stress–slip model of fiber reinforced plastics sheet–concrete interfaces with a simple method." Journal of Composites for Construction, 9(1), 52-62.

[15] Zhou, Y.W., Wu, Y.F., and Yun, Y.C., 2010, "Analytical modeling of the bond–slip relationship at FRP-concrete interfaces for adhesively-bonded joints." Composites Part B: Engineering, 41(6), 423-433.

[16] Wu, Y.F., and Jiang, C., 2013, "Quantification of bond-slip relationship for externally bonded FRP-to-concrete joints." Journal of Composites for Construction, 17(5), 673-686.

LIST OF NOTATIONS

E_f = elastic modulus of FRP
F = external load applied to FRP in the single shear pull out test
L_f = bond length of FRP
$s(x)$ = slip distribution along the longitudinal direction x
s_0 = relative slip between FRP and concrete at the loaded end
t_f = thickness of FRP
α = parameter in the bond-slip relationship governing the shape of the bond-slip curve
β = parameter in the bond-slip relationship governing the shape of the bond-slip curve
$\varepsilon_f(x)$ = tensile strain of FRP along the longitudinal direction x
$\tau(x)$ = bond stress of FRP along the longitudinal direction x

LIST OF CAPTIONS FOR TABLES

LIST OF CAPTIONS FOR FIGURES

Table 1 — Specimen detail and test results of EB-FRP joints

Specimen ID	Epoxy interlocking/grooving				Peak load kN (kips)	Average α value mm (in.)	Average β value mm (in.)
	Spacing mm (in.)	Width mm (in.)	Depth mm (in.)	Filling material			
F-1	50 (2)	3 (0.12)	4.8 (0.19)	Epoxy	65.02 (14.62)	0.1949 (0.008)	39.47 (1.573)
F-2	50 (2)	3 (0.12)	4.9 (0.19)		64.87 (14.58)		
F-3	50 (2)	3 (0.12)	5.0 (0.20)		57.02 (12.82)		
U-1	50 (2)	3 (0.12)	4.9 (0.19)	Wax	29.74 (6.69)	0.1115 (0.004)	43.11 (1.697)
U-2	50 (2)	3 (0.12)	5.0 (0.20)		31.50 (7.08)		
U-3	50 (2)	3 (0.12)	5.0 (0.20)		37.69 (8.47)		
C-1	-	-	-	-	34.0 (7.64)	0.1002 (0.0039)	37.94 (1.494)
C-2	-	-	-	-	-		
C-3	-	-	-	-	-		

Table 2 — Material properties

Product		Property	Value
Concrete substrate		28-day cylinder strength, MPa (ksi)	34.5 (5.0)
		28-day split tensile strength, MPa (ksi)	3.62 (0.53)
		Width, mm (in.)	152 (6)
		Thickness, mm (in.)	152 (6)
		Length, mm (in.)	533 (21)
CFRP plate		Bond length L_f, mm (in.)	381 (15)
		Width b_f, mm (in.)	51 (2)
		Ultimate strength, MPa (ksi)	2790 (405)
		Tensile modulus, GPa (ksi)	155 (22,480)
		Ultimate strain (%)	1.8
		Nominal thickness, mm (in.)	1.5 (0.06)
Epoxy	Tyfo® S	Tensile strength, MPa (ksi)	72.4 (10.5)
		Tensile modulus, GPa (ksi)	3.18 (461)
		Elongation capacity (%)	5.0
	Tyfo® TC	Tensile strength, MPa (ksi)	22.7 (3.3)
		Tensile modulus, GPa (ksi)	1.2 (174)
		Elongation capacity (%)	1.88

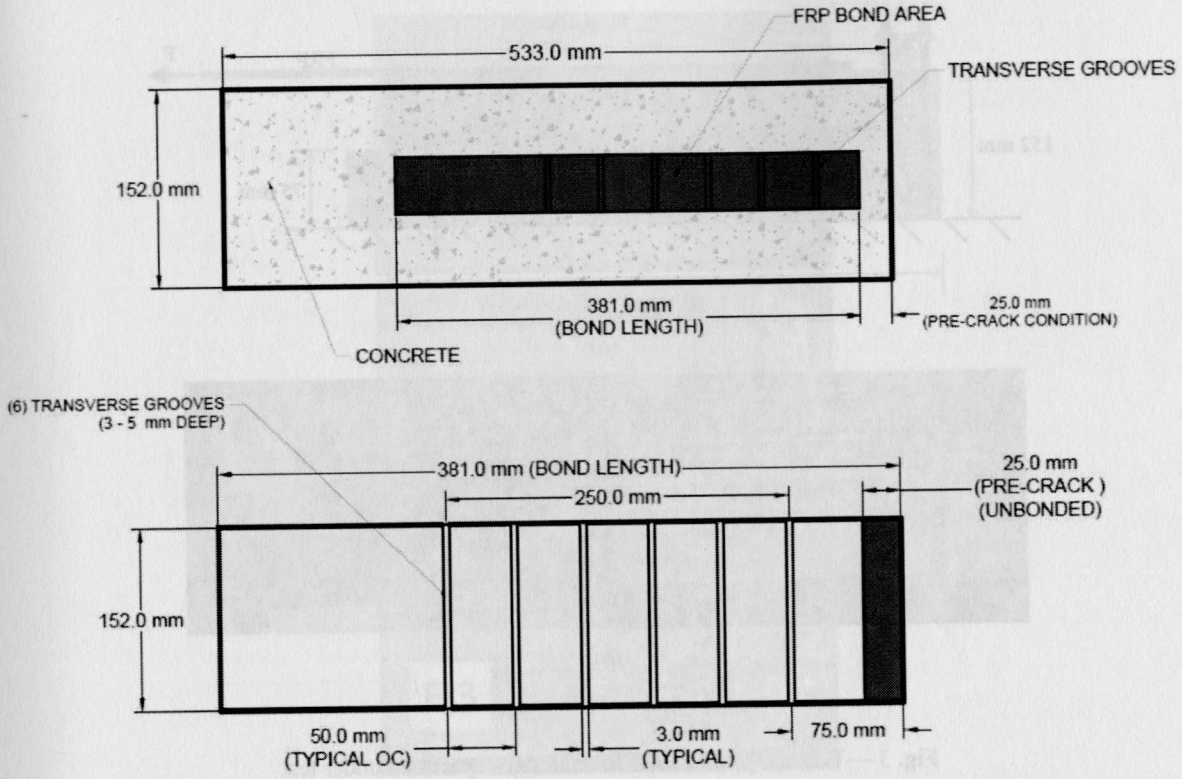

[1 mm = 0.0394 in]

Fig. 1 — Grooves and pre-crack condition dimensions of specimens

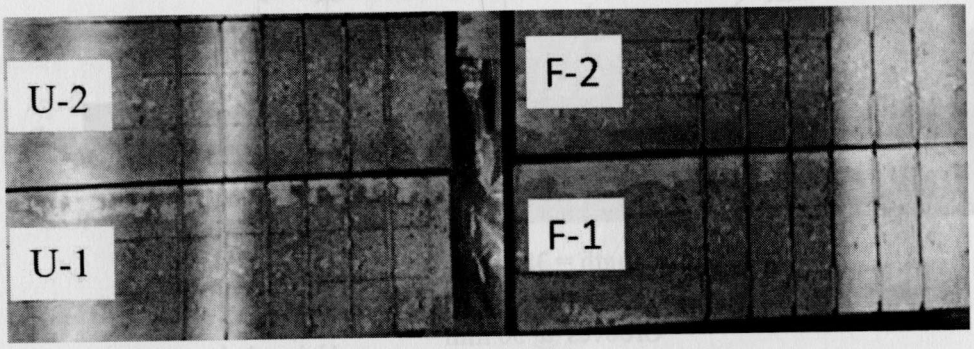

Fig. 2 — Waxed filled (U) and unfilled (F) specimens

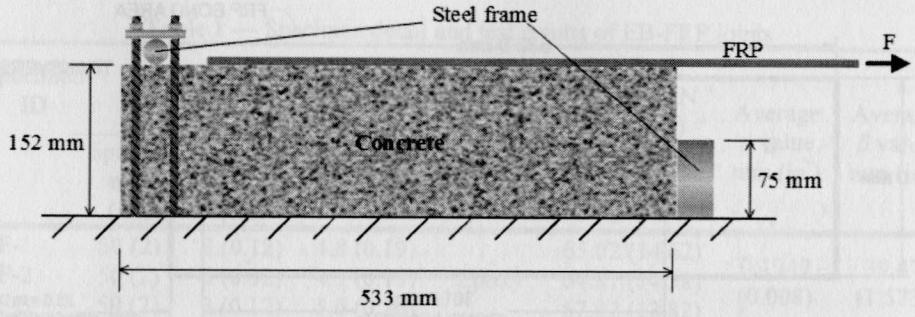

(a)

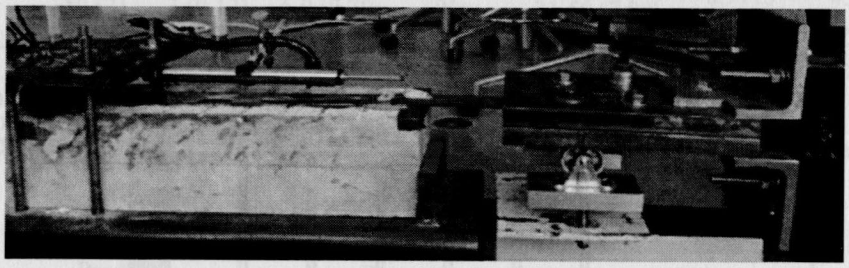

(b)

[1 mm = 0.0394 in]

Fig. 3 —Test setup: (a) schematic and (b) a specimen under test

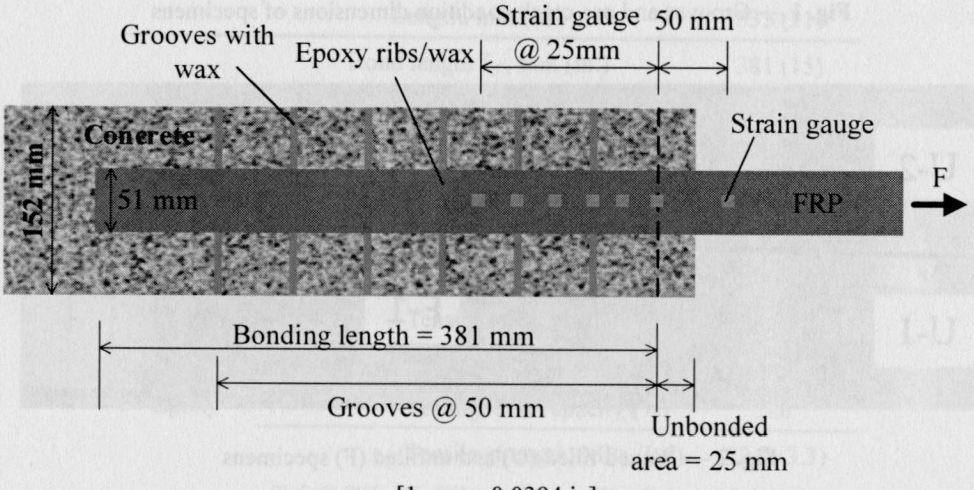

[1 mm = 0.0394 in]

Fig. 4 — Strain gage locations

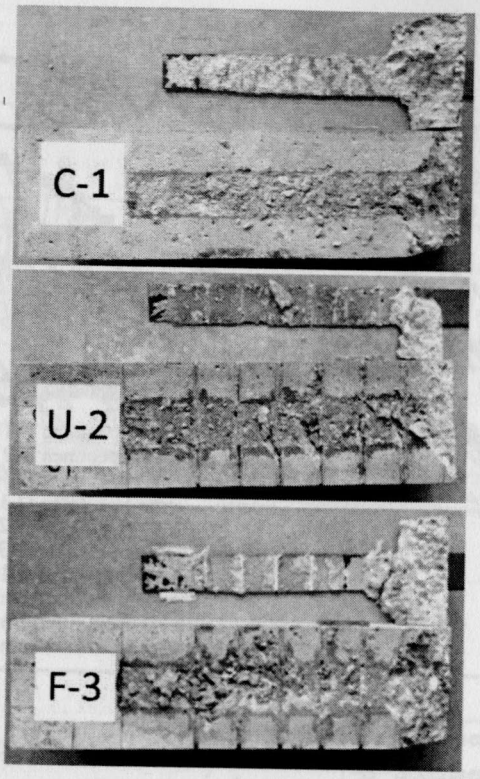

Fig. 5 —Typical failure modes

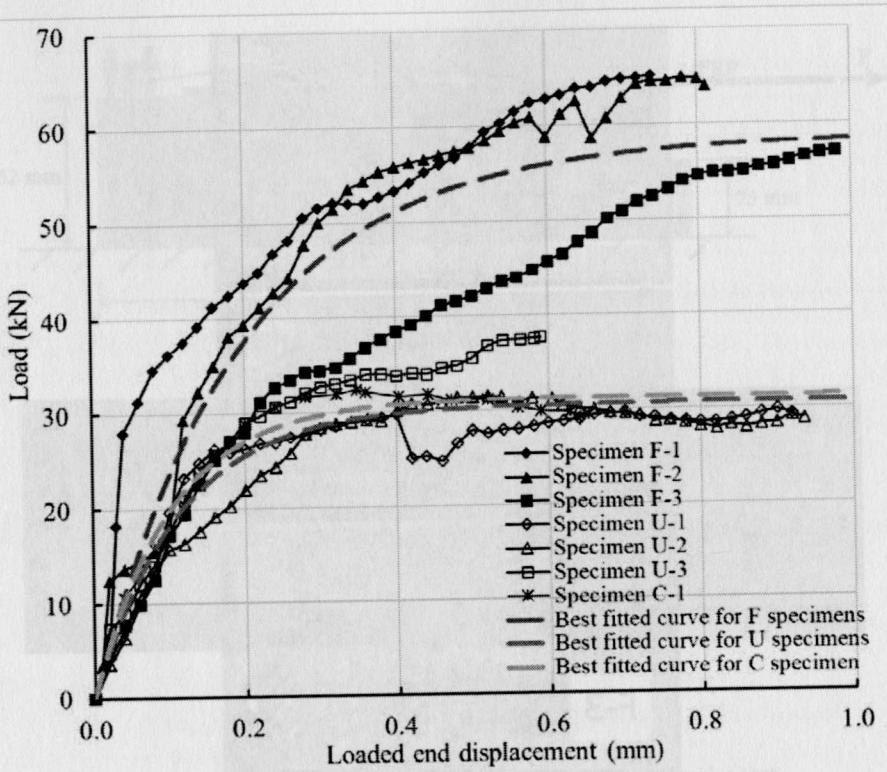

[1 mm = 0.0394 in; 1 kN = 224.809 lbs]

Fig. 6 — Load-displacement curves for specimens

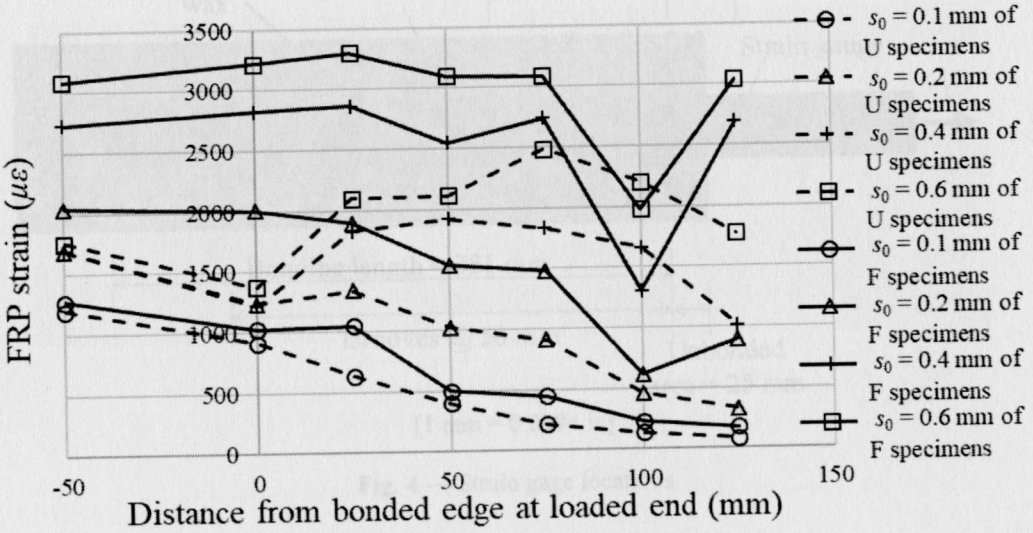

[1 mm = 0.0394 in]

Fig. 7 — Strain distributions of specimens

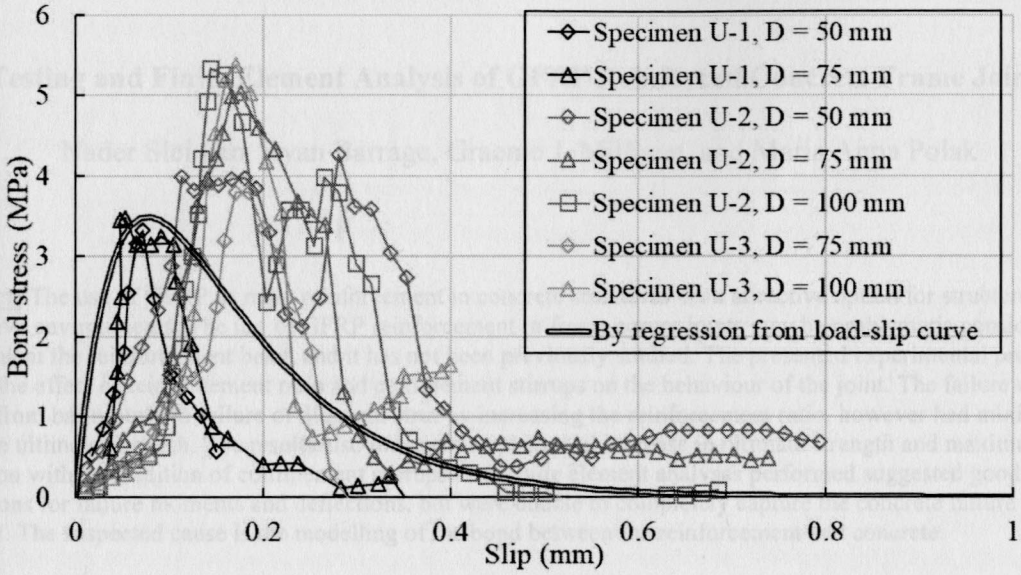

(a) Unfilled specimens

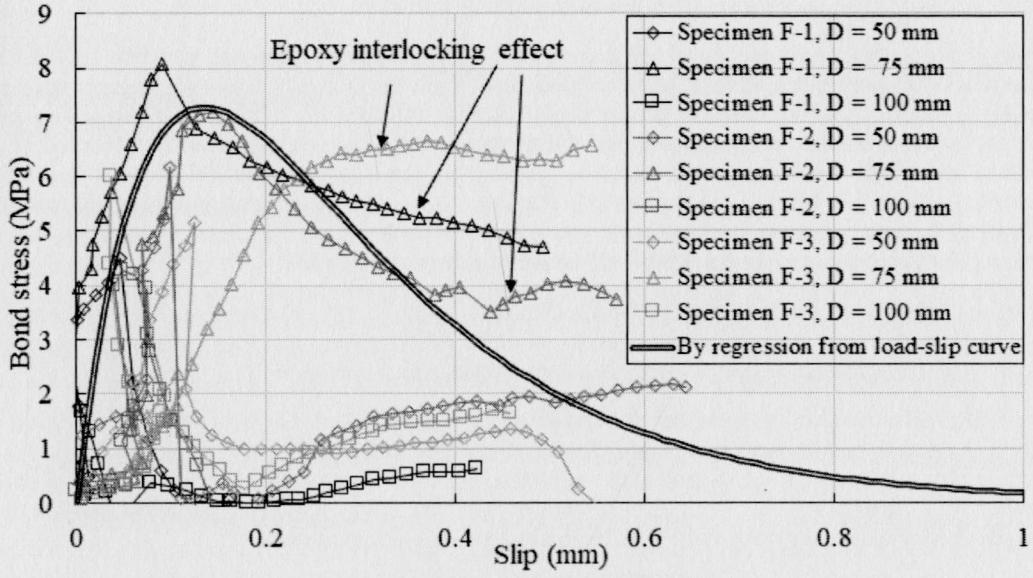

(b) Epoxy interlocking specimens

[1 mm = 0.0394 in; 1 MPa = 145.038 psi]

Fig. 8 — Bond-slip relationship (D is the distance from loaded end)